Triglyceride content and fatty acid composition in mice: quantification with 7.0T MRI

Benjamin Leporq[1], Simon Auguste Lambert[1,2], Francois Cauchy[1,3], Imane Boucenna[4], Pierre Colinart[4], Maxime Ronot[1,5], Valerie Vilgrain[1,5], Valerie Paradis[1,6], and Bernard Edgar Van Beers[1,5]

[1]Center of research on inflammation, Paris 7 University; INSERM U1044, Paris, France, [2]BHF Centre of Excellence, Division of Imaging Sciences and Biomedical Engineering, King's College London King's Health Partners, St. Thomas' Hospital, London, United Kingdom, [3]Department of HPB and liver transplantation, Beaujon University hospital Paris Nord, Clichy, France, [4]Matière et systèmes complexes, Paris 7 University; CNRS UMR 7057, Paris, France, [5]Department of Radiology, Beaujon University hospital Paris Nord, Clichy, France, [6]Department of Pathology, Beaujon University hospital Paris Nord, Clichy, France

Introduction: An increased dietary intake of fat, particularly polyunsaturated fatty acids (PUFAs) has been related to an increased risk of breast, prostate and colon cancers (1,2). Whereas the determination of adipose tissue fat composition provides objective information about fat intake (3), few MRI methods have been developed to quantify fatty acid composition and these latter only concern clinical systems (2-5). On preclinical systems, two problems need to be addressed: first, solve the chemical ambiguity in the reconstruction linked to the increase of B_0 inhomogeneities at higher field and, second, to combine shorter echo spacing with high spatial resolution. This work report a MRI method able to quantify both fat content and fatty acid composition on preclinical systems at 7.0T.

Material and Method: ***MR acquisition*** **-** MRI data were collected on a Bruker Pharmascan 7.0T system (Bruker, Ettlingen, Germany) equipped with a 300 $mT.m^{-1}$ shielded gradient set and a ^1H transmit-receive quadrature coil. A 2D multiple spoiled gradient echo sequence with bipolar readout gradients and synchronized with the respiration was used. 16 echoes were acquired (first echo: 1.58 ms; echo spacing: 0.74 ms). The acquisition parameters were: TR: 900 ms; hermitian pulse: 20°, receiver BW: 300 KHz, 8 signal averages, FOV: 45 mm^2, acquisition MX: 128^2, 20 axial slices of 1 mm thick. Phase and magnitude images were recorded. ***Images reconstruction*****:** To decrease overall computing time, pixel included in the background and air cavities were suppressed with a mask built from the magnitude images by using an active contour. Phase images were unwrapped before the reconstruction of complex images by adding multiples of ± 2π when absolute jumps between consecutive elements of a phase-time array were greater than or equal to a jump tolerance of π radians. By using a model including: a complex field map summarizing both off-resonance and R_2* effects; water and 8 fat resonances each expressed according to the number of double bound (ndb) and the number of methylene interrupted double bound (nmidb) (7) and a complex error map accounting for the phase error and the amplitude modulation caused by the bipolar readout gradients (6), parametric maps of proton density fat fraction (PDFF), saturated (SFA), monounsaturated (MUFA) and polyunsaturated fatty acids (PUFA) fraction were derived. The optimization procedure was performed with a non-linear least square fit using a multi-start Levenberg-Marquardt algorithm. ***In vitro study***: Validations were performed (i) on calibrated monodispersed fat-water emulsions with weight fat fraction included between 0 and 60% and (ii) on vegetable oils whose theoretical fatty acid composition was derived from fatty acid mass composition. ***Animal study***: The feasibility was evaluated on mice with two diets giving different fatty acid uptake: high fat diet (SFA: 176.9 $g.Kg^{-1}$, MUFA: 121 $g.Kg^{-1}$ and PUFA: 32.6 $g.Kg^{-1}$) and fructose diet (SFA: 8.9 $g.Kg^{-1}$, MUFA: 22.4 $g.Kg^{-1}$ and PUFA: 70.9 $g.Kg^{-1}$).

Results: Linear regressions showed strong agreement between PDFFs and weight fat fractions on emulsions (y = 0.98 x - 0.33, R^2= 0.99) and between ndb and nmidb quantified with MRI and the theoretical values derived from oil composition (y = 0.99 x + 0.012, R^2 = 0.99 and y = 0.95 x - 0.06, R^2 = 0.99 ndb and nmidb respectively. In vivo, significant differences in visceral adipose tissue fatty acid composition were found according to the diet. SFA were significantly higher in the high fat diet group than in the fructose diet group ($p<0.01$) whereas MUFA and PUFA were significantly lower in the high fat diet group than in the fructose diet group ($p<0.01$ and $p<0.05$ respectively).

Conclusion: Phase unwrapping before the reconstruction of complex images allows to solve the chemical ambiguity. The bipolar acquisition permits to combine a short echo spacing with a spatial resolution suitable for mice imaging. Phase and magnitude errors linked to bipolar gradient can be accounted by including a complex error map in the model. Our results shows that it possible to simultaneously quantify both fat content and fatty acid composition with 7.0T MRI on mice and to follow diet effects on fat content and fatty acid compositions in mice.

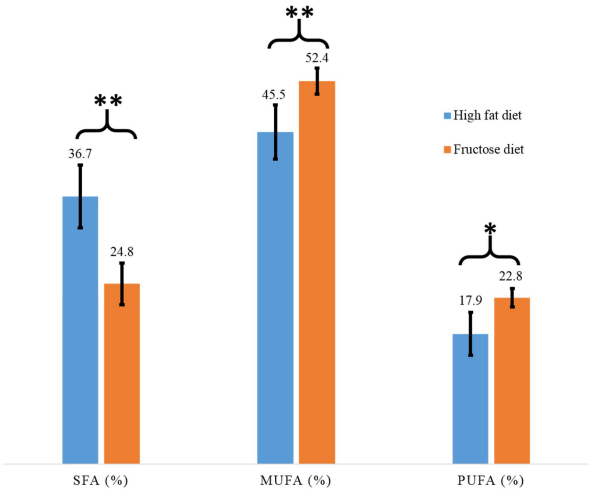

Fig.1 *Fatty acid composition of visceral adipose tissue (fraction of SFA, MUFA and PUFA according to the diet. In high fat diet, visceral adipose tissue is significantly more saturated than in fructose diet ($p < 0.01$). Both MUFA and PUFA are lower in high fat diet ($p < 0.01$ and 0.05 respectively) than in fructose diet.*

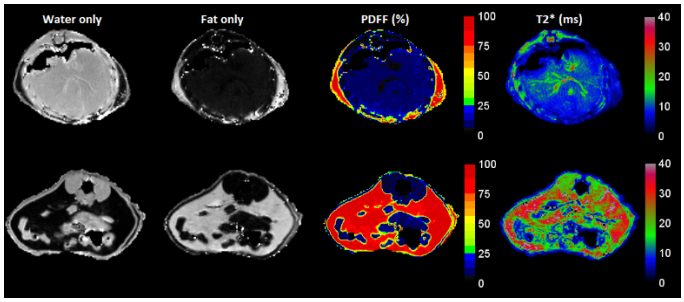

Fig.2: *Water and fat only images and parametric maps (PDFF and T_2*) computed with our method. Images are acquired on a high fat diet mouse and presented at two different slice levels. Mean PDFF and T_2* in liver are 9.1% and 8.0 ms respectively.*

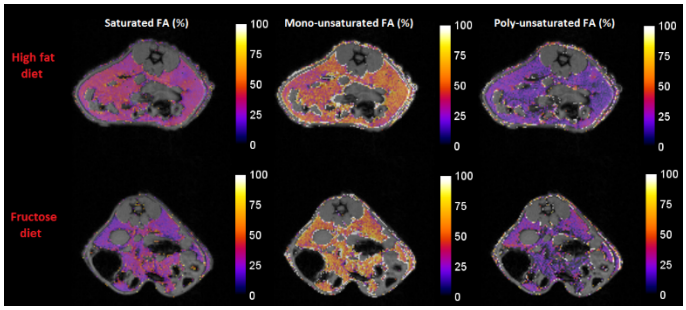

Fig.3*: Fatty acid composition maps (fraction of SFA, MUFA and PUFA) of visceral fat in two mice with different diets (high fat diet (upper row) and fructose diet (lower row).*

References :

(1) Theodoratou E *et al*. Am J Epidemiol 2007;166:181-195
(2) Jones R *et al.* Mol Cell Biochem 2003;253:141-149.
(3) Baylin A et al. Am J Clin Nutr 2002;76:750-757
(4) Bydder M *et al*. Magn Reson Imaging 2011;29:1041-1046.
(5) Berglund J *et al*. Magn Reson Med 2012;68:1815-1827.
(6) Peterson P *et al*. Magn Reson Med 2013;69:688-697.